Journal of Mining and Environment (JME) Published online

Shahrood University of Technology

Journal of Mining and Environment (JME)

Journal homepage: www.jme.shahroodut.ac.ir

Iranian Society of Mining Engineering (IRSME)

Evaluation of Ground Conditions to Enhance Rock Support in Underground Mine Excavations at Nkana Mine's Synclinorium Area

Victor Mutambo1*, Barnabas Mpaka[1], Pardon Sinkala[1], and Matheus Ipinge[2]

1. Department of Mining Engineering, School of Mines, University of Zambia, Lusaka, Zambia
2. Department of Civil and Mining Engineering, Faculty of Engineering and Information Technology. University of Namibia, Ongwediva, Namibia

Article Info

Received 2 April 2025

Received in Revised form 18 July 2025

Accepted 29 August 2025

Published online 29 August 2025

DOI: 10.22044/jme.2025.16018.3084

Keywords

Synchlinorium

Excavation stability

Ground control

Anchor system

Geological structures

Abstract

This study evaluates rock mass ratings, rock strength parameters, and the geological structures of the dominant rock units alongside a quantitative assessment of the performance of various anchor systems for enhanced ground support in mine excavations located within the Synclinorium area. This region is notable for its complex, folded, and mineralized formations. The deeper levels of the synclinorium are characterised by poor ground conditions, faults, and shear zones. Stress induced by mining activities worsens the situation. These factors have significantly impacted the stability of excavation. Fall-of-ground (FOG) incidents have exhibited a concerning increase over the past nine years. This trend necessitates a thorough investigation into the factors contributing to it. Our research employed empirical methods for rock mass classification, specifically utilising Barton's Q system and Bieniawski and Scanline mapping of geological structures along the crosscut walls at a 1.50 m elevation. We conducted borehole logging and pull-out tests to evaluate the working and ultimate capacities of rock bolt anchors deployed in the excavations. Borehole cores were analysed for geological formations, colour, and grain size. The findings indicate that excavations in areas with mined-through rock and stone necessitate urgent and intensive roof support to stabilise the surrounding rock mass, thereby enhancing standing time. Additionally, we identified joint patterns, joint orientations, and the various stresses affecting the surrounding rock mass in the crosscuts. The above highlights the importance of geological data in the design of effective ground control and support mechanisms. Pull-out testing conducted at the 3360 level recorded a 28.6% failure rate in primary development despite very competent ground.

1. Introduction

Nkana underground Mine has been in operation since 1930 when the first shaft was sunk at the Central Shaft. The area is predominantly characterised by the Nkana syncline. The orebody structure of the mine exhibits complex folding with both anticlines and synclines extending from south to north along a 1.3 km strike. The Synclinorium refers to the highly folded mineralized area at the keel of the Nkana Syncline currently extending from sections 1100 South (SOB) to zero (Central) below 3140ft Level at SOB and 3360ft Level at Central Shaft as shown in Figure 1 [1,2].

The Synclinorium is characterised by a complex geology with four main lithologies: South Orebody (SOB) Shale, Hanging Wall Argillite (HWA), Near Water Sediments and Upper Quartzite (UQ), all folded with varying thicknesses. The economic mineralization of copper-cobalt is concentrated along the North East (NE) limb of a north-westerly plunging synclinorium which forms part of the Chambishi–Nkana region [3,4]. The complex nature of the orebody at any mine such as the Synclinorium, dictates the use of different mining methods to suit the existing structures [5, 6]. At deeper levels, the host rocks are marked by complex folding, jointing and shearing that affect ground control and rock support. The mine also faces challenges related to mine-induced seismicity primarily due to the progressive accumulation of high-stress levels in the rock mass surrounding

Corresponding author: vmutambo@unza.zm (V. Mutambo)

excavations as they are expanded through mining. As mine development proceeds to deeper levels, the challenges associated with seismicity have intensified. Peter [7] explains that the mechanics of rock support are complex, and there are no models that can fully elucidate the interaction of various support components within a rock support system. When evaluating the ground medium, certain factors have a significant effect on the stability of jointed rock mass such as the initial in-situ stress-strain state and its change patterns, the mechanical behaviour of the rock mass in response to changing stress fields, and the shape and size of excavations [8]. Their study focused more on the mechanical properties of rocks rather than on the types of rock formations. The quality, orientation and dip of the rock mass in excavations significantly impact the stability of underground openings [9, 10].

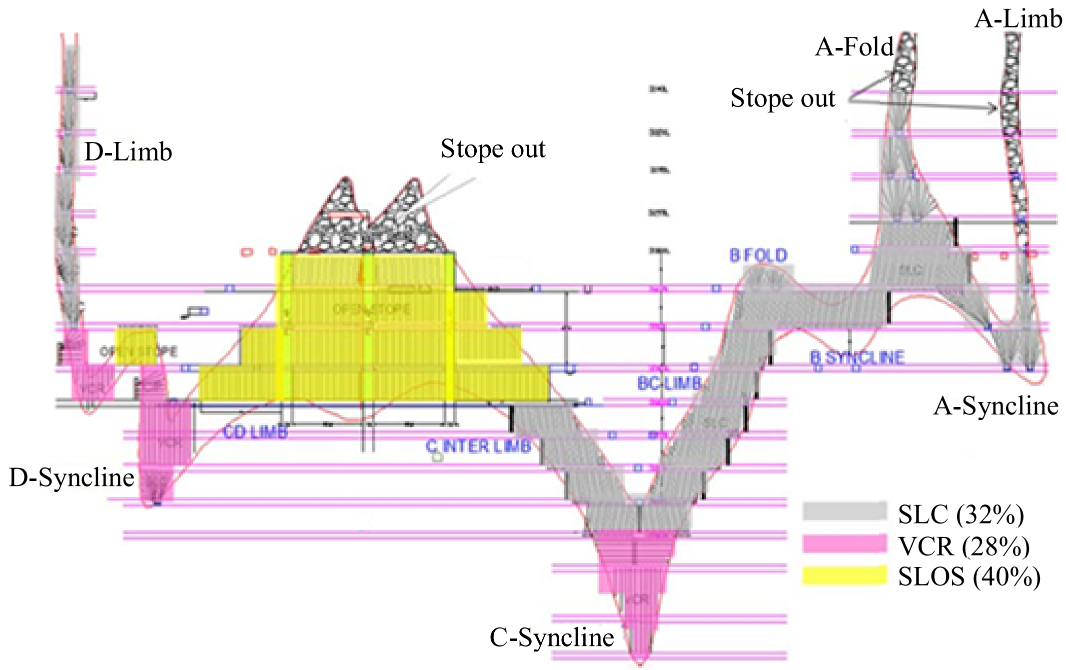

Figure 1. Section of the Synclinorium taken at 4800S

The effects of joints and the size of failure zones in rock masses near excavations particularly in the absence of support have been noted [9]. Protosenya and Vilner [11] established that geological and core logging methods should be employed when describing the composition of rock masses including shear zones and faults. There are at least six major complex folds labelled A-F arranged in echelon from east to west with their plunges undulating erratically. A noticeable flattening of the plunge occurs in barren gap areas which are associated with basement 'highs'. In contrast, the corresponding steepening of the plunge is observed off the flanks of the barren gaps. The folds are tightly compressed, exhibiting well-developed attenuation of limbs, crumpling of bedding planes, axial plane cleavage and axial plane shearing. The presence of faults and shear zones in mining excavations affects the stability of the excavation [12]. The excavations in the weak rocks should be supported to prevent premature failure. Such support may involve metal grids [13]. Tunnels driven through different rock type formations require an estimation of the initial type of support to maintain their stability [14]. Discontinuities, joints and their spacing in the rock mass surrounding mine excavations also influence the stability of the ground [15]. According to Ghorbani et al. [16] and Noroozi et al. [17], factors contributing to ground failure modes include the state of stress, groundwater pressure, induced stresses, seismic events, the orientation of discontinuities, the presence of geological structures, the size, shape, and location of tunnels, mining sequencing and groundwater conditions. The rock mass quality, tunnel size and in-situ stresses contribute to deformation [18]. In deeper levels of the synclinorium, the rock mass is characterised by high in-situ stress and mine-induced seismicity, further complicating rock support. Increasing mine depth is associated with sudden ground failure and deformation in rock mass structures [19,20]. When predicting the stability of surfaces in the open stope mining method, Mikaeil et al. [21] and Sharifi et al. [22] emphasised the need to incorporate stability graph parameters that include hydraulic radius, stability number, and related stability factors. Other factors affecting tunnel stability are stochastic fracture networks, rock mass properties, ground and water pressure [17].

Peter [7] explains that rock mass failure in excavations occurs when induced stress surpasses the peak strength of the rock mass. The induced stresses and geological structures affect the stability of excavations [23,24]. Mine-induced seismicity arises from the progressive build-up of high-stress levels in the rock mass surrounding excavations. Over the past nine years of operation in the synclinorium area, rock falls have been the leading cause of 32 fatal accidents. According to Mutambo and Mukuka [25], rock bursts and failures in seismically active mining blocks are exacerbated by the presence of geological and geotechnical structures. A thorough understanding of rock mass classification, geological structures and the general geotechnical environment is essential for addressing the challenges posed by the deeper underground environment of the synclinorium mine and for enhancing rock support in mine excavations. This study aims to determine detailed rock mass ratings for various rock formations, map geological structures and conduct pull tests on support systems to identify areas that require enhanced rock support. While some research has been conducted on identifying geological structures [26, 27, 28, 29], there has been limited focus on assessing the physical properties of rock types and their associated formations [30, 31, 32, 33, 34, 35, 36]. Therefore, it is crucial to strengthen the geotechnical database at the Nkana synclinorium mine. A comprehensive understanding of rock mass structure is key to estimating the inherent properties of the rock mass, which can aid in predicting ground behaviour. This understanding allows for the assessment of instability conditions and failure mechanisms in the rock mass surrounding underground excavations. Mazraehli et al. [37] used a probabilistic methodology to determine the statistics of rock mass strength and deformation parameters based on the GSI for evaluating the stability of tunnels. Rafiee et al. [38] established that excavation stability should not be based solely on a factor of safety unless a probabilistic analysis is applied.

Diagnosing ground behaviour and potential failure mechanisms can ultimately guide the selection of appropriate design analysis tools for ground support systems.

2. Materials and Methods

In the article, we used empirical methods for rock mass classification, point load tests for determining the Uniaxial compressive strength (UCS) of rock sample cores, scanline mapping of geological structures, borehole logging and pull testing.

2.1. Empirical methods for rock mass classification

The rock mass classification was conducted to evaluate the estimates for underground tunnel support. We used Barton's Q system for rock mass classification because it is a more comprehensive approach that considers the physical properties of discontinuities [39]. This Q-system incorporates the Rock Quality Designation (RQD) which was developed by Deere [40] to quantify rock quality along with several other factors such as Jn (joint sets), Jr (joint roughness), Ja (joint alteration), Jw (water pressure) and SRF (stress reduction factor). The relationship between these variables is illustrated in Equations 1 and 2.

$$\mathrm{Q} = \frac{\mathrm{RQD}}{\mathrm{Jn}} \mathrm{x} \frac{\mathrm{Jr}}{\mathrm{Ja}} \mathrm{x} \frac{\mathrm{Jw}}{\mathrm{SRF}} \tag{1}$$

$$\mathrm{RQD} = \frac{\text{Sum of Core pieces} \geq 100\ \text{mm}}{\text{Drill cores Run(Total Core Length)}} \mathrm{x}\ 100 \tag{2}$$

Where J_n is the joint set number, J_a is the joint alteration number, J_r joint roughness number J_w joint water reduction factor, SRF is the stress reduction factor.

Bieniawski (1973) classification:

Bieniawski's classification gives a Rock Mass Rating (RMR) indicative of the quality of the rock mass. The RMR combines geologic characteristics of influence into one overall comprehensive index of rock mass quality. In this study, Bieniawski's 1989 [41] Rock Mass Rating (RMR) values were obtained from equation 3.

$$\mathrm{RMR} = \mathrm{Ln}(\mathrm{Q}) + 44 \tag{3}$$

Geological Strength Index (GSI):

This index was derived from evaluating the state of discontinuity surfaces, structure, and the lithology of the rock mass using the Hoek-Brown failure criterion [42,43]. It was estimated through visual inspection of mine excavation faces as well as borehole cores. The geological strength index is estimated as follows:

GSI≈ $RMR76$ ≈ $RMR89$ -5 for GSI ≥ 18 or RMR ≥ 23	(4)
GSI≈9InQ[1] + 44 for GSI < 18	(5)
$Q^1 = \frac{RQD}{Jn} x \frac{Jr}{Ja}$	(6)

RMR_{76} represents the RMR value applied by Bieniawski in 1976 with a maximum groundwater rating of 10. Similarly, RMR_{89} represents the RMR values applied by Bieniawski in 1989.

Where Q' = modified rock mass quality.

2.2. Mapping of geological structures

The Geological Society of London [44] and the International Society for Rock Mechanics (ISRM) [45] have proposed standards for collecting engineering geological data. Scanline mapping of geological structures was conducted to identify features such as joints, bedding planes, schistosity and folds. This mapping took place along crosscuts or tunnel walls at an elevation of 1.5 meters. Geological features were recorded along a stretched 100-meter tape with known centerline survey pegs used as reference points. A Brunton compass and a Crinol ruler were employed to measure the strike and dip of the geological contacts and structures. The joint data collected from underground was entered into an Excel spreadsheet compatible with DIPS software. In the DIPS spreadsheet, also referred to as the Grid Data View, the data is organized into a maximum of 40 rows and includes the following columns: two orientation columns, a quantity column, a traverse column, a distance column, and three sets of coordinates (Easting, Northing, and Elevation), along with three additional columns. To display the planes (great circles) for all planar data in the Dips file, the Sidebar options were used to select "Planes" and "Grid Data Planes," which ultimately show the great circles. Each great circle is represented by dip vectors on the Stereonet which indicate the maximum dip orientation of a plane and are orthogonal to the pole vector of that plane. The Dips software allowed the researchers to analyse and visualise joint data using the Stereonet feature.

2.3. Borehole logging

Geotechnical core logging involves detailed examination and description of rock samples obtained from boreholes onto log sheets [46, 47]. Borehole cores were examined for geological formations, colour and grain size. Geological structures like joints, bedding planes, folds and schistosity were also logged. Core angles and RQDs were also estimated using a crinol ruler, measuring tape, and a Brunton compass. Water and a brush were used for washing the core. In total, 10 boreholes were logged out of 16 boreholes of NQ core size (standard outer diameter size of the drill rod, approximately 60.3 millimeters), representing 60% of the population needed for mechanical rock property testing in rock formations such as foot wall sandstone (FSAN), footwall conglomerate (FCON), basal sandstone (BQ) and south orebody shale (SOB).

2.4. Pull-out testing

The Allowable Load Testing (ALT) method was used. It involved fixing a hydraulic pull tester to an anchor and pulling it until it fails [48,49]. This test determines the stress levels required for the structure to collapse. Anchor Testing was repeated five to eight times with the average being the final result. The pull-out test was used to measure the working and ultimate capacities of a rock bolt anchor. To make sure the bolt response during the test was minimal and predictable, high-strength, short-length (1.8 to 2.5 m) bolts were used. In this research, the required anchorage ranged from 8 to 10 tonnes. The anchors used for pull testing were double-ring split sets. The system for pulling the rock bolts consisted of a hollow-center hydraulic ram and a reaction frame. The hydraulic ram had a travel range of 50 mm. The loading system shall apply a force that deviates by no more than 5° from the long axis of the bolt during the test. A load transducer was used to measure the loading on the rock bolt. A dial gauge was used to measure the displacement of the rock bolt head. It had an accuracy of 0.025 mm, a resolution of 0.013 mm and a range of 50 mm. For every 100 double-ring cable bolts installed, 5% should be subjected to pull testing, representing a target of 20 double-ring. However, in this research, 23 double-ring cable bolts were tested in the area of interest representing 105%.

3. Results

3.1. Rock mass parameters and ratings

Results of the study indicate that the rock mass ratings (RMRs) for the samples of Basal Quartzite (BQ), Foot Wall Conglomerate (FCON), South Orebody Shale (SOBS) and Hanging Wall Argillite (HWA) rock formations compared well with Barton's Q system RMR ranges, except for Foot Wall Sandstone (FSAN) which was out of range. The RMR for FSAN at 78 did not fall in Barton's Q system RMR range of 60-70. This shows a lack of confidence in the available data in the database and requires consistency in data collection.

The uniaxial compressive strength (UCS) for each rock formation had a linear relationship with the geological strength index (GSI). The UCS also had a notable linear relationship with rock quality designation (RQD) and joint spacing which are the two other parameters that are closely associated. Table 1 summarizes the rock parameters and ratings based on the formation.

The detailed ratings for individual rock formations studied and analyzed for RMRs are outlined in Tables A2-A7, while Table 2 shows statistical analysis of measured rock parameters.

Table 1. Values of rock mass parameters at Nkana Mine.

Rock unit	RQD Range	IRS Range	RMR Range	RMR Description	Q Range	Q Description
Basal Quartzite	80-100	100-50	70-80	Good	18-55	Good-very Good
Lower conglomerate	60-80	50-100	38 - 58	Poor- Fair	1 - 5	Poor - Fair
F/W quartzite	40-80	50-100	60 - 70	Fair -Good	6 - 18	Fair - Good
SOB Shale	40-68	50-100	40 - 60	Poor- Fair	1 - 6	Poor - Fair
HWA	40-70	50-100	40 - 60	Poor- Fair	1 - 6	Poor - Fair

Table 2. Statistical analysis of measured rock parameters

		H/W Argillite	F/W Sandstone	Basal Quartzite	F/W Conglomerate	South Ore Body
N	Valid	6	6	6	6	6
	Missing	0	0	0	0	0
Mean		80.83	69.17	119.33	63.17	45.17
Median		67.50	70	82.50	66.00	52.50
Mode		43[a]	35[a]	53[a]	32[a]	20[a]
Std. Deviation		45.031	28.456	75.251	25.779	18.346
Sum		485	415	716	379	271

a. Multiple mode exists. The smallest value is shown

3.2. Mapping of geological structures

Joints mapped in the study area of 3510 and 3960 levels in the crosscuts intersecting the limbs and the base of the syncline fall in the southeast, with the joint sets generally dipping to the northeast at the average dip of 65 while the joints on the 3960-level dip at 60° on average to the southeast with their concentration in the north of the Stereonet. Figures 2 and 3 show contoured Stereonets of crosscuts in the SE limb of the Synclinorium at the base. As seen from Figure 2, the Joint density concentrations are in the north and are generally dipping southwards.

The Joint density concentration in Figure 3 lies in the northeast and generally dips in the south and southwest. The dip of the joints mapped at the base of the syncline on the 3960 level in Table 3 is also steeply dipping, averaging 65°. As expected, folded areas of the structure are associated with steep joint planes.

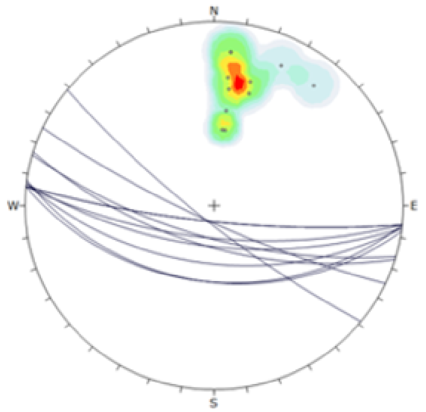

Colour	Density Concentrations
	0.00 - 3.20
	3.20 - 6.40
	6.40 - 9.60
	9.60 - 12.80
	12.80 - 16.00
	16.00 - 19.20
	19.20 - 22.40
	22.40 - 25.60
	25.60 - 28.80
	28.80 - 32.00
Maximum Density	31.24%
Contour Data	Pole Vectors
Contour Distortion	
Contour Circle	10%
Maximum Mode	Pole Vectors
Vector Count	11(11 Entries)
Hemisphere	Lower
Projection	Equal Angle

Figure 2. Stereonet for 3960 Level -750 Cross Cut.

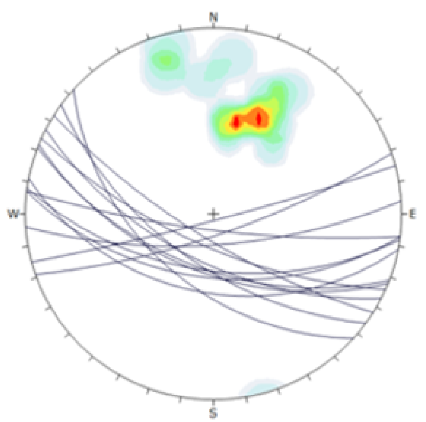

Colour	Density Concentrations
	0.00 - 2.40
	2.40 - 4.80
	4.80 - 7.20
	7.20 - 9.60
	9.60 - 12.00
	12.00 - 14.40
	14.40 - 16.80
	16.80 - 19.20
	19.20 - 21.60
	21.60 - 24.00
Maximum Density	23.64%
Contour Data	Pole Vectors
Contour Distortion	
Contour Circle	10%
Maximum Mode	Pole Vectors
Vector Count	14(14 Entries)
Hemisphere	Lower
Projection	Equal Angle

Figure 3. Stereonet for 3960 Level-710 Cross Cut.

Table 3. Joint set orientation data for 3960L/750 and 710 Cross Cuts.

3960L/750			3960L/710		
ID	DIP	Dip Direction	ID	DIP	Dip Direction
1	80	186	1	57	201
2	65	197	2	71	176
3	45	186	3	80	187
4	70	186	4	86	165
5	55	187	5	52	187
6	45	188	6	75	212
7	65	187	8	70	204
8	70	196	9	61	207
9	80	186	10	55	202
10	80	219	11	77	161
11	80	205	12	44	191
			13	56	188
			14	49	222

A haulage inspection walk along the 3360 level of Synclinorium mine revealed a sidewall excavation meant for a waiting place or refuge bay. The hanging wall had two joint sets crisscrossing along strike and across strike as shown in Figure 4. A highly stressed timber set installed for support is tilted, leaving major joint sets unsecured over a large span of hanging wall.

The joint orientation and different stresses acting on the surrounding rock mass are illustrated and evaluated in Figure 5.

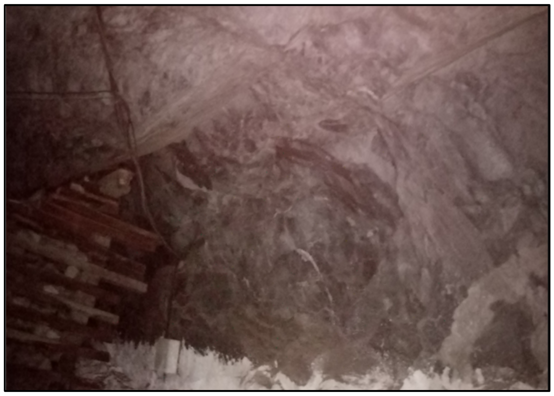

Figure 4. Timber pack under a jointed and stressed rock mass (Source - Picture taken at Nkana Synclinorium underground, 3360 haulage level).

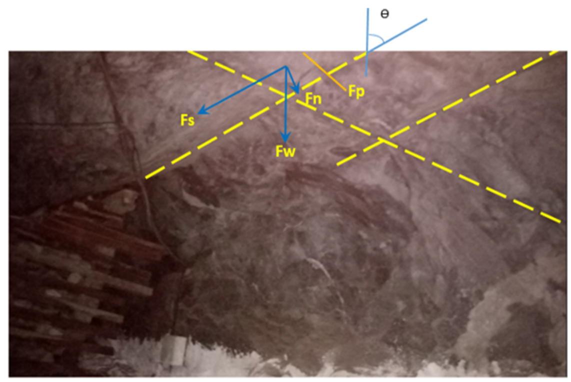

Figure 5. Analysis of joint patterns and joint plane inclinations (Nkana Synclinorium, 3360 haulage level).

This helps in understanding the distribution of forces acting in a stressed rock. Hence, any passive support like props or timber packs will be effectively applied. Figure 6 shows intense folding and shearing in a cross-cut mined through the ore shale formation at 3435 level of the synclinorium underground.

Shear displacement and stress forces acting on a synclinal structure in 810 crosscut on the 3860 level of Synclinorium mine are outlined in Figure 7.

Forces acting on the fold limbs (Figure 6): Fs = Shear Displacements; Fn = Stress forces perpendicular to limbs. Diamond drilling and geological mapping conducted at the site have revealed large-scale folds and small localized folds. These folds are not only characterised by joints but also by shear displacements along the limbs towards the fold axis and stress forces perpendicular to the limb (Figure 8). This affects the stability of the folded rock mass.

Figure 9 shows fresh black shale with joint planes parallel to the fine laminations on the 3760 level.

Figure 6. Highly folded and sheared mineralized shale at Nkana Synclinorium underground, 3435 Level. *The approximate position of the fold axis is presented by the yellow arrow. The blue pen gives the approximate distance between white dolomitic bands.

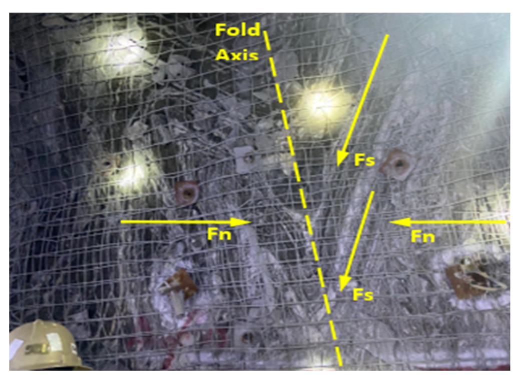

Figure 7. Highly folded and mineralized sheared shale supported at Nkana Synclinorium underground, 3860 Level.

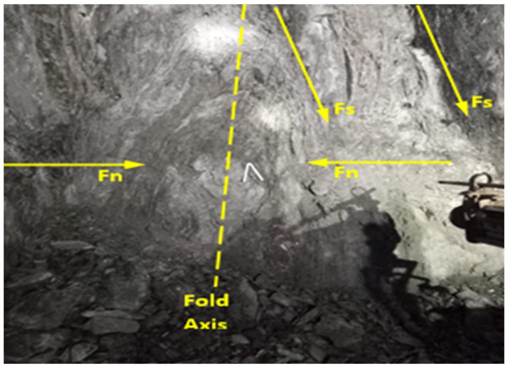

Figure 8. Highly folded and weathered mineralized Shale. White 1 m 4 Folds Plastic Ruler - folded half picture is 25 cm long.

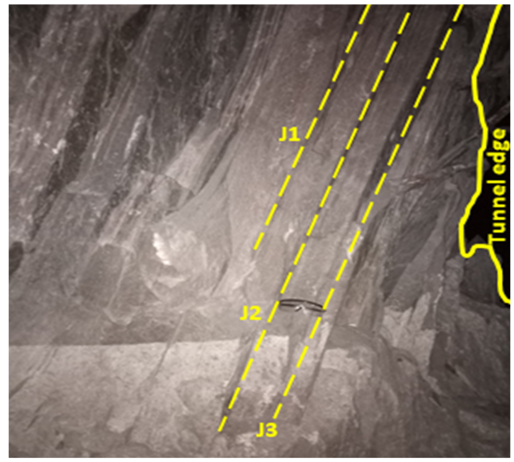

Figure 9. Fresh laminated and jointed barren Shale at Nkana Synclinorium underground, 3760 Level. The length of the safety goggles is about 20 cm.

3.1. Evaluation of ground support standards at Synclinorium Mine

Pull Testing was done in selected mine excavations to provide a quantitative measure of the relative performance of different anchor systems. By standard, every development excavation was subjected to pull testing. Pull-test data for each site at which the cable bolts were tested was plotted on graphs to determine the failure rate and assess the standard of installation practices. Table 4 shows the types of support that were tracked for quality tests weekly at Synclinorium Mine.

Table 4. Recommended ground support testing frequency and specifications.

Element	Testing Methods	% of elements to be tested	Frequency	Required anchorage (tons)
Groutable Rock bolt	Pull test -full column	5 % of installed bolts	Weekly	10
Split set	Pull test- full anchor	5 per batch	Weekly	8
Shotcrete	Cube Tests			
	Flow test			
	Depth Probe		Per application	
	Panel Test		Per 50 m^3 placed	
	Insitu cores			
Cable bolt	Load in cable bolt – SMART cable	5 % of installed bolts		
Timber support	Load in packs			
Backfill load				

Figure 10 shows a plot of the results of failure loads against id samples for pull-out test 1 conducted on 3360 level haulage, while Table 5 shows the detailed parameters used in the pull-out test and corresponding remarks.

Seven rock bolts (split sets) were subjected to pull-out testing with a threshold strength set at 8 tonnes. Five borderline cases in light blue passed at a load of 8 tonnes and the two red ones failed at loads of 6 and 7 tonnes respectively.

Table 6 shows a layout for the pull-out test carried out on 3360 main haulages, including recommendations for split set size and rock mass characteristics.

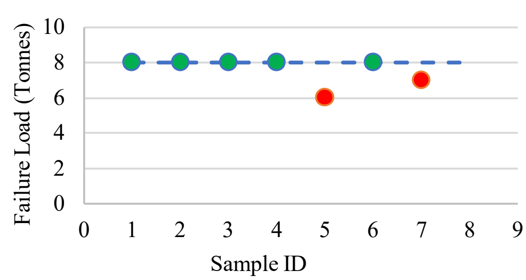

Figure 10. Pull-out test 1 graph (3360 haulage level).

Table 5. Detailed parameters used for pull-out test 1 results.

Test No.	Distance (m) Ref. Peg No. (C1583)	Wall	Bolt Length	Bond Type	Displacement (mm)	Test to 8 Tonne		Remarks
						Pass	Fail	
SS1	65.7	East	2.4 m	Friction	None	8		PND
SS2	65.7	West	2.4 m	Friction	None	8		PND
SS3	68.3	East	2.4 m	Friction	None	8		PND
SS4	90.4	West	2.4 m	Friction	None	8		PND
SS5	117.3	West	2.4 m	Friction	> 50mm		6	FND
SS6	121.8	West	2.4 m	Friction	None	8		PND
SS7	123.4	East	2.4 m	Friction	> 50mm		7	FND

*PND – Pass no displacement, FND- Fail noticeable difference

Table 6. Pull-out test 1 preparation.

Project	3360L _Main haulage
Pull test no:	1
Anchor type:	Split set; 2.4 m long
Rock bolt diameter:	46 mm
Hole diameter:	43 mm
Tunnel size:	4.5 m x 4.5 m
Rock mass classification	Basement Schistose: Fair to good rock mass with little persistent joints Bedded rock mass parallel to excavation axis Foliations exposed on the western side wall intersected by moderate joints RMR range of (41- 60) fair rock mass. UCS = 50 - 100 MPa
Date of installation	15/08/2022 – 16/09/2022
Date of test:	16.08.2023

Preparation for pull-out test 1 involved understanding the project site, the types of rock present, the type and diameter of rock bolts and the size of the tunnel. Figure 11 shows the plan indicating the locations of pull-out tests conducted on the 3360 main haulage, along with the associated results.

The results from a pull test 1 performed on seven (7) double ring split sets, installed along the grade line of the 3360-level main haulage were as follows: two (2) bolts failed and five (5) passed the test. This represents a pass rate of 71% and a failure rate of 29%.

In Figure 12, the graph indicates 3 failed pull-out tests for test 2 (in red for a threshold set at 10 tonnes). Five tests passed at the load of 10 tonnes.

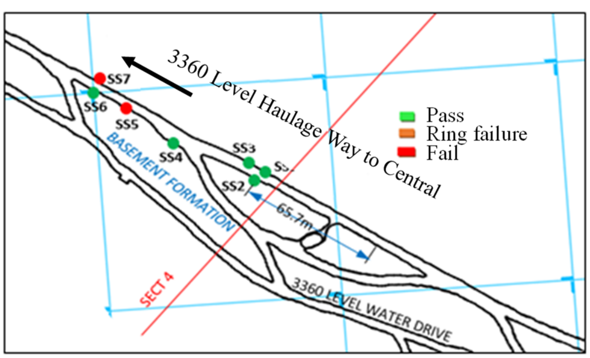

Figure 11. Pull-out test 1 - Double Ring Split Sets.

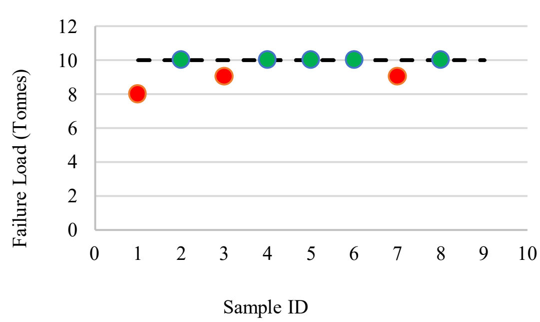

Figure 12. Pull-out test 2 graph (3960 Level- 1150 mN Loader Drive North).

Detailed parameters used for the pull-out test 2 at the site are shown in the appendix in Table 10A. The 3 failed tests recorded were attributed to the split set rings. The layout for the pull test carried out on 3960 level 1150N Loop Loader Drive including recommendations for split set size and rock mass characteristics, is shown in the Appendix (Figure A1 and Table A7 respectively). Figure 13 shows a graph of pull-out test 3 results conducted at 3510 L/820 XC.

All eight pull-out tests depicted in Figure 13 were successful. Three of these tests were conducted at loads of 8 tonnes which met the compliance limit. The remaining tests produced results that exceeded this limit. Pull-out test 3 was performed at the 3510 level/820XC as indicated in the plan shown in Figure 14.

Table 7 shows the results of Pull-Test 3 conducted on 3510/20XC level - C Interlimb, while Table 8 shows the overall number of tests conducted and the ratings.

All 8 tests passed the pull test as indicated by the results in Table 7. When the opening was left unsupported, the maximum displacements in the modeled drives reached 12 cm. After installing the bolts, the maximum displacements were reduced to 9 cm. Out of the twenty-three (2) tests conducted, the two (2) and three (3) failures come from sites 1 and 2, respectively.

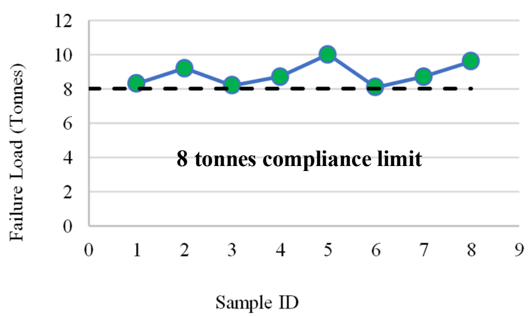

Figure 13. Pull-out test 3 results.

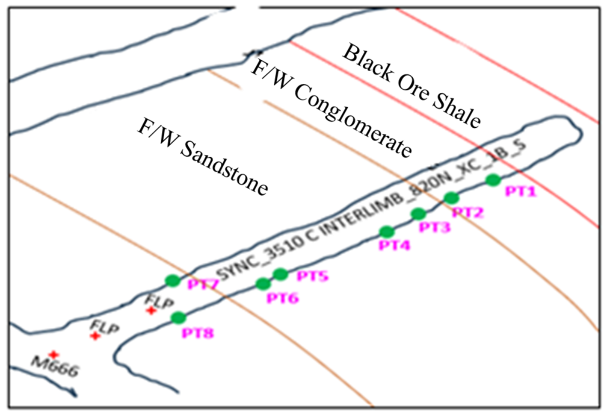

Figure 14. Pull-out test 3 Location- 3510/820XC – C Interlimb.

Table 7. Parameters used with the corresponding pull-out test 3 results.

Test No.	Distance from Ref. Peg M6665	Wall	Bolt Length	Bond Type	Displacement (mm)	Test to 8 Tonnes		Remarks
						PASS	FAIL	
PT1	41	South	2.4 m	Friction	None	8.3	-	Pass
PT2	37	South	2.4 m	Friction	None	9.2	-	Pass
PT3	34	South	2.4 m	Friction	None	8.2	-	Pass
PT4	31	South	2.4 m	Friction	None	8.7	-	Pass
PT5	23	South	2.4 m	Friction	None	10	-	Pass
PT6	22	South	2.4 m	Friction	None	8.1	-	Pass
PT7	15	North	2.4 m	Friction	None	8.7	-	Pass
PT8	14	South	2.4 m	Friction	None	9.6	-	Pass

Table 8. Number of tests conducted and the ratings.

		Frequency	Percent	Valid Percent	Cumulative Percent
Valid	**Pass**	18	78.3	78.3	78.3
	Fail	5	21.7	21.7	100
	Total	23	100	100	

4. Discussion

4.1. Ground instabilities

In this study, understanding the causes of ground instability in the Synchlinorium area was essential for implementing effective mitigation strategies. The following interrelated factors were identified as prime factors for ground instability in the Synclinorium: rock mass properties, geological discontinuities and inadequate ground support and reinforcement. This study has established the link between ground instabilities associated with poor rock mass ratings, specifically in the FWQ, where instability in the excavations has taken the form of side wall and roof slabbing/scaling, pillar spalling and corner crushing in drives. The RMRs for BQ, FCON and FSAN are outside the acceptable range. This highlights the necessity for ongoing updates to the Synclinorium mine rock mass parameters through regular data collection from underground mapping, laboratory tests and core logging. The sandstone, which underlies much of the host rock for copper mineralization on the footwall side, has a fine grain size and is generally slightly weathered. However, it is part of a highly stressed and folded zone characterised by discontinuities such as joints and bedding planes. Excavations through sandstone typically involve secondary development near the orebody, requiring urgent and extensive roof support to stabilize the surrounding rock mass for improved standing time. In addition, falls of ground from the roof are in the form of rock slabs/blocks and prisms/wedges resulting from the intersection of two or three joint sets, respectively. This study has established the need to share mutually beneficial geological and geotechnical information between geologists and mining engineers in the Nkana Mine using the Synclinorium as a case study. The timely provision of geological information on geological structures and joints is key in applying effective ground control and support mechanisms around mine excavations. For example, the geological information on thin and highly weathered ore units intersecting the cross-cuts and geological contact showed a greater possibility of instability in the said excavations. Geologists, therefore, provide essential data that drive successful ground control and excavation support systems, thereby reducing ground failures and collapses [50,51].

The unit that meets the stability parameters is the Footwall Conglomerate with a strength value of 105 MPa and an RMR of 65. BQ is the strongest of all the listed rock types, with a strength value of 178 MPa and an RMR of 82. It can effectively stand on its own for extended periods with minimal support. Ninety percent of the BQ rock mass is found in primary developments such as haulages and water drainage drives. The samples in this study were classified according to the standard Unconfined Compressive Strength (UCS) classifications by Bieniawski, Bernede and ISRM (1979) [52,53]. The comparisons made between RMRs (Table A1) for the core samples used in this study and Barton's Q system range (Table A2) revealed that only the RMRs of SOB and HWA are within the acceptable limits of Barton's Q system, while BQ, FCON and FSAN fall outside this range. This underscores the ongoing need to update the Synclinorium mine rock mass parameters through regular underground mapping, laboratory testing and core logging. The UCS of rock is used for determining the failure characteristics and mechanical behaviour of rocks under different loading conditions [54, 55, 56, 57, 58, 59, 60].

4.2. Influence of major joints

The dipping of major joints which is oblique to the limbs and syncline in the study areas, significantly impacts the stability of the already folded and sheared geological structures. The Stereonets presented in Figures 2 and 3 illustrate density patterns that represent joint sets, which generally exhibit a southwest dip direction as most of the great circles of the joint planes face this direction. It is important to note that the poles shown in the density patterns are situated close to the perimeter of the Stereonet and farther from the center. In contrast, the great circles representing the joint planes are located nearer to the centre of the Stereonet where the dip is approximately 90 degrees. In permanent excavations, such as haulages or refuge cubbies, it is essential to diligently map and analyze major joint planes that may affect ground stability to understand potential failure planes. A practical example of this is shown in Figure 5 which illustrates a rock mass where several geological discontinuities are presented along a haulage at the Synclinorium mine. An examination of this figure reveals that only one of these discontinuities (indicated by a heavy broken line running downward to the left) poses a threat to the stability of the system. The forces acting on this potential failure plane include:

- FW: the total weight of the rock wedge (W);
- FN: the normal force acting across the plane (N);
- FS: the shear force acting along the plane (N);
- FP: the total force due to fluid pressure (if present) within the rock mass (N).

The condition for unstable equilibrium is:

$$F_S = \mu(F_N - F_P) \quad (7)$$

where μ is the coefficient of friction which is effective along the potential failure plane. The requirement for the stability of the slope can be expressed as follows:

The coefficient of friction (μ) between two dry rock surfaces is approximately 0.7. This value may be lower if the potential failure plane contains soft filling material. According to Hoek et al. [42,43], [14] and [26], mapping the geological structure is crucial for identifying structural planes in the rock mass. These planes can either fall or slide from the excavation boundary if they are not adequately supported. In Figures 2 and 3, the two cross cuts 750 XCUT1 and 710 XCUT1 were chosen for analysis based on their higher density of joints and their central location within the study area. The finding on the effect of discontinuities on the stability of excavations is supported by Turanboy [15].

4.3. Implications of pull test results

In this study, rock bolts were subjected to rigorous testing to determine their failure rate, reliability and safety in underground excavations.

The failure rate data provides insights into the performance and durability of the cable bolts under operational conditions. The results obtained from these tests offer a valuable indication of the adherence to best practices and standards in the installation procedures. Out of three test sites (sites 1, 2, and 3) conducted, only test site 3 recorded a 100 % pass rate for all anchors subjected to an 8-tonne load. Test sites 1 and 2 recorded two (2) and three (3) failures respectively. The failure at Site 1 can be attributed to substandard installation practices. This aligns with earlier findings by Kim et al. [61], Barton [62], and Coimbra et al. [63], who established the impact of poor installation practices on anchor performance and bearing capacity in different ground conditions. Overall, the results of the pull-out tests highlight a lack of consistency among the personnel involved in the installation of cable bolts. Additionally, it indicated compromised inspection processes.

5. Conclusions

This study evaluated the geotechnical parameters of rock mass, the geological structures of the dominant rock units and the performance of various anchor systems with a view to enhancing ground control and support of mine excavations in the synclinorium area. Empirical methods for rock mass classification, point load tests to determine the Uniaxial compressive strength (UCS) of rock sample cores, scanline mapping to determine geological structures, borehole logging and the allowable pull testing method to determine anchor failure applied. The key findings of the study are that the ground instabilities in the area are due to the interaction between the excavation and rock structure (rock mass strength and discontinuities, joint and bedding planes), stress and seismicity. Furthermore, the geological structures such as folds (anticlines/synclines) have significantly contributed to rock instability around underground excavations in the Synclinorium. This study has further revealed that rocks characterized by discontinuities and folding have weaker mechanical rock properties, with strengths of 47 MPa for Shale and 65 MPa for Argillite, both linked to ground instability. The sandstone which underlies a significant portion of the host rock for copper mineralization on the footwall side exhibits a relatively high strength of 116 MPa. However, it is also marked by discontinuities such as joints and bedding planes necessitating urgent and intensive roof support to stabilize the surrounding rock mass for improved standing time.

Pull tests evaluated the load-bearing capacity of anchors to establish their reliability in the excavations. Pull-out tests yielded unsatisfactory results regarding the integrity of installed anchors in relatively strong ground. These failures, along with noticeable displacements of the rock bolts, are attributed to substandard installation practices.

This study recommends continuous updating of the geotechnical and geological databases to inform the design of excavations. In addition, simulating ground conditions around excavations, both before and after the installation of anchorage systems provides valuable insights into the interaction between reinforcement support and the surrounding rock mass, particularly concerning ground movement and induced stresses.

We suggest that future research be directed towards the possible use of Artificial Intelligence and Machine Learning for predicting failures in the mine excavations and the surrounding rock medium based on historical geotechnical and geological databases.

Conflict of Interest Statement

The authors declare that they have no known competing financial interests or personal relationships that could have appeared to influence the work reported in this paper.

Acknowledgments

The authors would like to acknowledge the partial financial support covering field work from the University of Zambia, School of Mines and declare that there are no competing financial interests to influence the work reported in this paper.

Data availability

Data will be made available on request.

References

[1]. Jordaan, J. (1961). Nkana. In: Mendelsohn, F. (Ed.). The Geology of the Northern Rhodesian Copperbelt. MacDonald, London, pp. 297–328.

[2]. Bard, P.G., Jordaan, J. (1963). Some structural features associated with the Rokana orebodies. In: Lombard, J., Nicolini, P. (Eds.). Stratiform Copper Deposits in Africa. 2nd Part: Tectonics. Association of African Geological Surveys, Paris, pp.179–191.

[3]. Brems, D., Muchez, P. H., Sikazwe, O. & Mukumba, W. (2009). Metallogenesis of the Nkana Copper- Cobalt South Orebody, Zambia. *Journal of African Earth Sciences.* 55(1): 185-196.

[4]. Muchez, P. H., Brems, E., Clara, A., Cleyn, D., Lammens, A., Boyce, D., Muynck, D., Mukumba. W., Sikazwe, O. (2010). Evolution of Cu–Co mineralizing fluids at Nkana Mine, Central African Copperbelt, Zambia. *Journal of African Earth Sciences*. 58: 457-474.

[5]. Jankovic, M., et al. (2011). Mining methods for complex ore deposits. *Mineral Processing and Extractive Metallurgy Review*, 32(2), 101-118. https://doi.org/10.1080/08827500802378626.

[6]. Poulsen, H. (2004). Mining Methods at Complex Ore Bodies. *Minerals Engineering*, 17(4): 585-595

[7]. Peter, K. K., Ming, C. (2012). Design of rock mechanics support system under rock burst condition. *Journal of Rock Mechanics and Geotechnical Engineering*, 4 (3): 215–227.

[8]. Hoek, E., & Brown, E. T. (1980). Empirical Strength Criterion for Rock Masses. *Journal of Geotechnical Engineering*, 106: 1013–1035.

[9]. Boghdady, B. Y., Mohamed, E. I. A. (2016). The evaluation of the Effect of Rock Joints on the Stability of Underground Tunnels. Journal of Rock Mechanics, 3, 1790-1799.

[10]. Mutambo, V., Kangwa, S., Fisonga, M. (2022). Mining method selection for extracting moderately deep ore body using analytical hierarchy process at Mindola sub-vertical shaft, Zambia. *Cogent Engineering*. 9(1): 1-21. DOI: 10.1080/23311916.2022.2062877

[11]. Protosenya, A., Vilner, M. (2021). Assessment of excavation intersections' stability in jointed rock masses using the discontinum approach. *The Mining-Geology-Petroleum Engineering Bulletin and the authors*. pp. 137-147. DOI: 10.17794/rgn.2022.2.12.

[12]. Palmstrom, A., Stille, H. (2015). Rock Engineering, 2nd ed.; Institution of Civil Engineers, London, UK, 456 P.

[13]. Nehrii, S. H., Nehrii, T. O., Piskurska, H. V., Fesenko, E. V., Pavlov, Y. Y., & Surzhenko, A. M. (2021). Substantiating Parameters of Reinforced Rock Supports. *Journal of Mining and Environment,* 12(4): 953-967.

[14]. Mikaeil R., Bakhshinejad H., Shaffiee Haghshenas S., Ataei M. (2019). Stability Analysis of Tunnel Support System Using Numerical and Intelligent Simulations (Case Study: Kouhin Tunnel of Qazvin-Rasht Railway), Rudarsko-geološko-naftni zbornik. *The Mining-Geology-Petroleum Engineering Bulletin*, 34(2): 1-11. DOI: 10.1177/rgn.2019.2.1

[15]. Turanboy, A., Ülker, E., & Burak Küçüksütçü, C. (2020). A New Stability Approach Using Probabilistic Profile along Direction of Excavation. *Journal of Mining and Environment*, 11(1), 1-20.

[16]. Sharifzadeh, M, Ghorbani, M., Yasrobi S., 2017. Observation-based design of geoengineering projects with emphasis on optimization of tunnel support systems and excavation sequences. In *Rock Mechanics and Engineering.* Ed. Feng X.T., Volume 4: excavation, support and monitoring. Taylor and Francis Group, London, UK. 486 P.

[17]. Noroozi, M., Rafiee, R., & Najafi, M. (2018). Stability analysis of support systems using a coupled FEM-DFN model (Case study: a diversion tunnel at Lorestan dam site, Iran). *Journal of Mining and Environment*, 9(2): 485-497.

[18]. Rehman, H., Shah, A., Mohd Hashim, M. H. B., Khan, N. M., Ali, W., Shah, K. S., ... & Adeel, M. B. (2022). Investigating Effect of Tunnel Size, Rock Mass Conditions, and In-Situ Stresses on Stability of Tunnels. *Journal of Mining and Environment*, 13(4): 973-987

[19]. Rahimi, B., Sharifzadeh, M., Feng, X.T. (2020). Ground behaviour analysis, support system design, and construction strategies in deep hard rock mining justified in Western Australian mines. *Journal of Rock Mechanics and Geotechnical Engineering.* 20: 1-20.

[20]. De la Vergne, J. (2008). Hard Rock Miner's Handbook. Ed. 5., Stantec Consulting, Edmonton, Alberta, Canada, 314P.

[21]. Mikaeil R., Shaffiee haghshenas S., Ataei M. (2020). Statistical and intelligent modeling of underground open stope stability based on the stability graph method. *Journal of Analytical and Numerical Methods in Mining Engineering*, 10(24): 137-148., DOI: 10.29252/anm.2019.1629

[22]. Sharifi M., Mohammadi S., Ataei M., Kakaie R. (2021). Statistical and intelligent modeling of underground open stope stability based on the stability graph method. *Journal of Analytical and Numerical Methods in Mining Engineering*, 11(26):47-58, DOI: 10.29252/ANM.2020.14645.1454

[23]. Ngoma, K., Mutambo, V. (2020). Factors Influencing Ore Recovery and Unplanned Dilution in Sublevel Open Stopes. Case Study of Shaft No.4 at Konkola Mine, Zambia. Curr. *World Environ.* 15 (Special issue 1):31-46.

[24]. Ghorbani, M., Shahriar, K., Sharifzadeh, M., Masoudi, R. (2020). A critical review of the developments of rock support systems in high-stress ground conditions. *International Journal of Mining Science and Technology*, 30:555- 572.

[25]. Mutambo, V., Mukuka, M. (2024). Modified geomechanical dependant seismic monitoring arrangement for predicting rock bursts and failures in seismically active mining blocks at Mufulira mine. In: Korniyenko V., Lazar M (Eds). In Modern forms of development of resource-saving technologies for minerals mining and processing, Universitas Publishing, Petroşani, Romania, pp.119-127.

[26]. Pollard, D. D., & Aydin, A. (1988). Progressive fault growth and related damage zones. Geology, 16(8): 826829.

[27]. Tchalenko, J. S., & Kempton, P. D. (1988). Structural analysis of geological features. In: John son, R. E. (Ed.), Structural Geology. Wiley. pp 170–192

[28]. McClay, K. R. (1991). Structural geology: a new approach. *Earth-Science Reviews*, 30(1-2), 85-103

[29]. Nelson, C. R. (2001). Structural Geology. Oxford University Press, 698 P.

[30]. Hoek, E., & Brown, E. T. (1980). Underground excavations in rocks. Institute of Mining and Metallurgy, 384 P.

[31]. Goodman, R. E. (1989). Introduction to Rock Mechanics. Wiley, 657 P.

[32]. Hustrulid, W., & McCarter, M. (1996). Rock mechanics and tunnel design. Balkema.

[33]. Brady, B. H., & Brown, E. T. (2004). Rock Mechanics for Underground Mining. Springer.

[34]. Hoek, E., & Marinos, P. (2007). Estimating the friction angle of rock materials. *Tunneling and Underground Space Technology*, 22(3): 254-258.

[35]. Barton, N. (2002). Review of rock mass classification systems. In: Engineering Rock Mass Classification (pp. 1-24). Springer.

[36]. Lemann, J. P. (2014). Laboratory testing of rock properties. In: Rock Mechanics and Engineering Springer.

[37]. Mazraehli, M., Zare, S., & Idris, M. A. (2021). Stochastic Stability Analysis of Tunnels Considering Randomness of Rock Mass Properties. Journal of Mining and Environment, 12(4), 1123-1141.

[38.] Rafiee R., Ataei M., Kamali M., 2013, Tunnels stability analysis using binary and multinomial logistic regression (LR), *Journal of Geology and Mining Research*, 5(4): 97- 107.

[39]. Barton, N., Lien, R., Lunde, J. (1974). Engineering classification of rock masses for the design of tunnel support. *Rock Mech*. 6:183-236.

[40]. Deere, D.U.,1963. Technical description of rock cores for engineering purposes. *Rock Mechanics and Engineering Geology,* 1:16-22.

[41]. Bieniawski, Z.T., Bernede, M.J. (1979). Suggested methods for determining the uniaxial compressive strength and deformability of rock materials: Part 1. Suggested method for determining deformability of rock materials in uniaxial compression. *Int J Rock Mech. Min Sci. Geomech. Abstr.* 16:138 140.

[42]. Hoek, E., Kaiser, P.K., Bawden, W.F. (1995). Support of underground excavations in hard rock. A.A. Balkema Publishers, Rotterdam, Netherlands. 232P.

[43.] Hoek, E. (2011). Strength of rock and rock masses. *ISRM News J*. 2:4-16

[44]. Anon (1977). Description of rock masses for engineering purposes. Geological Society Engineering Group Woring Party Report. *Q. J. Eng. Geol. and Hydrogeol*. 10: 355-388.

[45]. International Society for Rock Mechanics (ISRM) Commission on Standardization of Laboratory and Field Tests. (1978). Suggested methods for the quantitative description of discontinuities in rock masses. *Int. J. Rock Mec. Min. Sci. & Geomec*. Abst. 15: 316- 319

[46]. Tims, S., Caté, A., LeRiche, A., & Saunders, E. (2024). Automated geotechnical logging of core box images using machine learning. *CIM Journal*, 16(1): 25–34. https://doi.org/10.1080/19236026.2024.2385269

[47]. Abzalov, M. (2016). Geotechnical Logging and Mapping. In: Applied Mining Geology. Modern Approaches in Solid Earth Sciences, vol. 12. Springer, Cham. https://doi.org/10.1007/978-3-319-39264- 6_6

[48]. Tucker, D. C., & Hughes, S. J. (2001). Design and testing of rock bolting systems in underground mines. *International Journal of Rock Mechanics & Mining Sciences*, 38(3): 377-392.

[49] Meyer, C. A., & Kleinke, K. (2000). Load testing of rock anchors in underground mines. Proceedings of the 2000 Symposium on the Practical Applications of Mining and Tunneling Techniques

[50]. More, C. G., O'Ferrall, Du Plessis, M. (2017). The influence of Geological Structures – an often-overlooked important aspect affecting the stability of operating mines. ISRM International Symposium Rock Mechanics for Africa AfriRock Conference, 2–7 October, Cape Town, Southern African Institute of Mining and Metallurgy.

[51]. Das, A.J., Mandal, P.K., Sahu, S.P. (2018). Evaluation of the Effect of Fault on the Stability of Underground Workings of Coal Mine through DEM and Statistical Analysis. *J Geol Soc India* 92: 732–742.

https://doi.org/10.1007/s12594-018-1096-2

[52]. Bieniawski, Z.T., Bernede, M.J. (1979). Suggested methods for determining the uniaxial compressive strength and deformability of rock materials: Part 1. Suggested method for determining the deformability of rock materials in uniaxial compression. *Int J Rock Mech. Min Sci. Geomech. Abstr.* 16: 138–140.

[53]. International Society for Rock Mechanics and Rock Engineering, ISRM. (1979). Suggested methods for determining the uniaxial compressive strength and deformability of rock materials, *Int J Rock Mech Min Sci*. 16:135-140.

[54]. Hajiabdolmajid, V., Kaiser, P., 2023. Brittleness of rock and stability assessment in hard rock tunneling. *Tunn. Undergr. Space Technol*. 18: 35-48.

[55]. Xia, Y., Zhou, H., Zhang, C., He, S., 2019. Wang, P. The evaluation of rock brittleness and its application: a review study. *Eur. J. Environ. Civil Eng*. 26: 239-279.

[56]. Meng, F., Wong, L.N.Y., Zhou, H. (2020). Rock brittleness indices and their applications in different fields of rock engineering. *J. Rock Mech. Geotech. Eng*. 13: 221-247

[57]. Zhang, X.P., Xie, W.Q., Cai, K.Y., Liu, Q.S., Wu, J., Li, W.W. (2021). Evaluation of rock muck using image analysis and its application in the TBM tunneling. Tunn. *Undergr. Space Technol. 113, 103974.*

[58]. Yagiz, S. (2008). Utilizing rock mass properties for predicting TBM performance in hard rock conditions. *Tunn. Undergr. Space Technol*. 23: 326-339.

[59]. Kahraman, S. (2001). Evaluation of simple methods for assessing the uniaxial compressive strength of rock. *Int. J. Rock Mech. Min. Sci*. 38: 981-994.

[60]. Hoek, E. (1966). Rock Mechanics - an introduction for the practical engineer Parts I, II and III. Series of special lectures in Mining and Metallurgy. *Mining Magazine* London. Pp: 1-56.

https://static.rocscience.cloud/assets/resources/learning/hoek/1966-Rock-Mechanics-

Introduction.pdf#:~:text=This%20paper%20is%20the%20text%20of%20three%20lectures,of%20Special%20University%20Lectures%20in%20Mining%20and%20Metallurgy

[61]. Kim, Y. J., Kim, J. H. & Lee, S. Y. (2008). Evaluation of the Effect of Installation Quality on Anchor Performance in Rock. *International Journal of Rock Mechanics and Mining Sciences*, 45(7):927–935.

[62]. Barton, R. B. (1975). Rock Support, Rock Bolts, and Ground Control. *Geotechnique*, 25(2): 131–165.

[63]. Coimbra, P. A. L. S. (2020). Assessment of Anchor Performance in Difficult Ground Conditions. *Rock Mechanics and Rock Engineering*. 53: 1525–1541.

Appendix A

Table A1. Rock Mass Ratings (RMRs) for rock samples at Synclinorium mine.

Rock unit	PLS Test (MPa)	RQD (%)	Joint spacing (cm)	RMR	GSI	Q
SOBS	47	62	20	58	59	25
HWA	65	75	170	70	62	43
FSAN	116	76	35	78	64	46
FCON	105	70	32	65	67	40
BQ	178	83	245	82	75	53

Table A2. RMRs used in this study versus Barton's Q system RMR ranges.

Formation	Logged samples	Barton's Q system	RMR Description
	RMR	RMR	
BQ	82	70 - 80	Good
FCON	65	38 - 58	Poor - Fair
FSAN	78	60 - 70	Fair - Good
SOB	58	40 - 68	Poor - Fair
HWA	70	40 - 70	Poor - Fair

Table A3. Detailed Rock Mass Rating for Shale (SOB).

Lithology	Item	Value	Rating
Shale (SOBS)	Point Load Index	47 MPa	12
	RQD	62%	11
	Spacing of discontinuities	20 cm	13
	Condition of discontinuities	-	15
	Groundwater	-	12
	Adjustment for joint orientation	-	-5
Total			58

Table A4. Detailed Rock Mass Rating for Hanging Wall Argillite (HWA).

Lithology	Item	Value	Rating
Hanging Wall Argillite (HWA)	Point Load Index	65 MPa	18
	RQD	75%	15
	Spacing of discontinuities	170 cm	20
	Condition of discontinuities	-	12
	Groundwater	-	10
	Adjustment for joint orientation	-	-5
Total			70

Table A5. Detailed Rock Mass Rating for Foot Wall Sandstone (FSAN).

Lithology	Item	Value	Rating
Foot Wall Sandstone (FSAN)	Point Load Index	116 MPa	14
	RQD	76%	15
	Spacing of discontinuities	35 cm	18
	Condition of discontinuities	-	21
	Ground water	-	15
	Adjustment for joint orientation	-	-5
Total			78

Table A6. Detailed Rock Mass Rating for Foot Wall Conglomerate (FCON).

Lithology	Item	Value	Rating
Foot Wall Conglomerate (FCON)	Point Load Index	105 MPa	15
	RQD	70%	14
	Spacing of discontinuities	32 cm	13
	Condition of discontinuities	-	16
	Groundwater	-	12
	Adjustment for joint orientation	-	-5
Total			65

Table A7. Detailed Rock Mass Rating for Basal Quartzite (BQ).

Lithology	Item	Value	Rating
Basal Quartzite (BQ)	Point Load Index	178 MPa	20
	RQD	83%	17
	Spacing of discontinuities	245 cm	21
	Condition of discontinuities	-	16
	Groundwater	-	13
	Adjustment for joint orientation	-	-5
Total			82

Table A8. Pull out test 2: Preparation layout.

Project:	3960L 1150mN Loop loader drive north
Pull test no:	2
Anchor type:	Split set; 2.4 m long
Rock bolt diameter:	46 mm
Hole diameter:	43 mm
Tunnel size:	4.5 m x 4.5 m
Rock Mass Classification:	Basal Sandstone – Lower Conglomerate rock unit Fairly competent rock and dry rock mass RMR fair rock unit. Estimated UCS of 150MPa and 45MPa, respectively Unfavorable joint orientation concerning the tunnel
Date of Installation	01/05/2021 – 29/06/2021
Date of test:	30.05.2023

Table A9. Rock Strength based on the Point Load Index test.

Rock type	Description	Equivalent UCS (MPa)
Basal Quartzite (BQ)	Extra strong	178
FW Sandstone (FSAN)	Strong rock	116
FW Conglomerate (FCON)	Very strong rock	105
HWA (Argillite)	Strong rock	65
SOB Shale (SOBS)	Medium Strong rock	47

Table 10A. Detailed parameters used in pull-out test 2 results.

Test No.	Distance (m) Ref. Peg No. (T5999)	Wall	Bolt Length	Bond Type	Displacement (mm)	Test to 10 Tonnes PASS	Test to 10 Tonnes FAIL	Remarks
SS1	1.4 m	North	2.4 m	Friction	None		8	PRFND
SS2	6.9 m	North	2. 4m	Friction	None	10		PND
SS3	6.9 m	South	2.4 m	Friction	None		9	PRFND
SS4	9.9 m	South	2. 4m	Friction	None	10		PND
SS5	12.9 m	North	2.4 m	Friction	None	10		PND
SS6	12.9 m	South	2.4 m	Friction	None	10		PND
SS7	24.4 m	South	2.4 m	Friction	None		9	PRFND
SS8	25.6 m	South	2.4 m	Friction	None	10		PND

*PND – Pass no displacement, PRFND- Pass ring failure no displacement

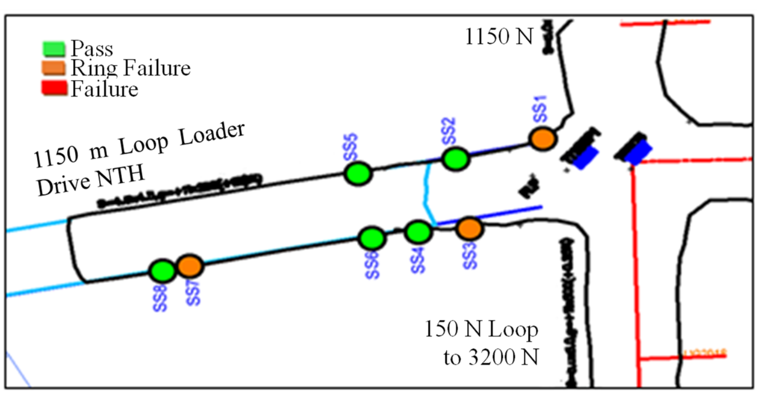

Figure A1. Pull out test 2 Location-3960/1150mN Loop Loader Drive North.

نشریه مهندسی معدن و محیط زیست
نشانی نشریه: www.jme.shahroodut.ac.ir
انجمن مهندسی معدن ایران
دانشگاه صنعتی شاهرود

ارزیابی شرایط زمین برای افزایش پشتیبانی سنگ در حفاری‌های معدن زیرزمینی در منطقه سینکلینوریوم معدن نکانا

ویکتور موتامبو[1]*، بارناباس مپاکا[1]، پاردون سینکالا[1] و ماتئوس ایپینگ[2]

۱ .گروه مهندسی معدن، دانشکده معادن، دانشگاه زامبیا، لوساکا، زامبیا

۲. گروه مهندسی عمران و معدن، دانشکده مهندسی و فناوری اطلاعات، دانشگاه نامیبیا، اونگودیوا

اطلاعات مقاله

تاریخ ارسال: ۲۰۲۵/۰۴/۰۲

تاریخ داوری: ۲۰۲۵/۰۶/۱۸

تاریخ پذیرش: ۲۰۲۵/۰۸/۲۹

DOI: 10.22044/jme.2025.16018.3084

کلمات کلیدی

سینکلینوریوم

پایداری گودبرداری

کنترل زمین

سیستم مهار

ساختارهای زمین شناسی

چکیده

این مطالعه، رتبه‌بندی توده سنگ، پارامترهای مقاومت سنگ و ساختارهای زمین‌شناسی واحدهای سنگی غالب را در کنار ارزیابی کمی عملکرد سیستم‌های مختلف مهار برای تقویت پشتیبانی زمین در حفاری‌های معدن واقع در منطقه سینکلینوریوم ارزیابی می‌کند. این منطقه به دلیل سازندهای پیچیده، چین‌خورده و معدنی خود قابل توجه است. سطوح عمیق‌تر سینکلینوریوم با شرایط نامناسب زمین، گسل‌ها و مناطق برشی مشخص می‌شوند. تنش ناشی از فعالیت‌های معدنی، وضعیت را بدتر می‌کند. این عوامل به طور قابل توجهی بر پایداری حفاری تأثیر گذاشته‌اند. حوادث ریزش زمین (FOG) در طول نه سال گذشته افزایش نگران‌کننده‌ای را نشان داده‌اند. این روند مستلزم بررسی کامل عوامل مؤثر در آن است. در تحقیق ما از روش‌های تجربی برای طبقه‌بندی توده سنگ، به ویژه با استفاده از سیستم Q بارتون و نقشه‌برداری بینیاوسکی و اسکن‌لاین از ساختارهای زمین‌شناسی در امتداد دیواره‌های متقاطع در ارتفاع ۱.۵۰ متر استفاده شد. ما آزمایش‌های ثبت گمانه و بیرون کشیدن را برای ارزیابی ظرفیت‌های کاری و نهایی مهارهای پیچ سنگی مستقر در حفاری‌ها انجام دادیم. مغزه‌های گمانه از نظر سازندهای زمین‌شناسی، رنگ و اندازه دانه‌ها مورد تجزیه و تحلیل قرار گرفتند. یافته‌ها نشان می‌دهد که حفاری‌ها در مناطقی با سنگ و صخره‌های استخراج‌شده، نیاز به پشتیبانی فوری و فشرده سقف برای تثبیت توده سنگ اطراف دارد و در نتیجه زمان توقف را افزایش می‌دهد. علاوه بر این، ما الگوهای درزه، جهت‌گیری درزه‌ها و تنش‌های مختلفی را که بر توده سنگ اطراف در برش‌های عرضی تأثیر می‌گذارند، شناسایی کردیم. موارد فوق اهمیت داده‌های زمین‌شناسی را در طراحی مکانیسم‌های مؤثر کنترل و پشتیبانی زمین برجسته می‌کند. آزمایش بیرون‌کشی انجام‌شده در سطح ۳۳۶۰، با وجود زمین بسیار مناسب، نرخ شکست ٪۲۸.۶ را در توسعه اولیه ثبت کرد.

نویسنده مسئول مکاتبات: vmutambo@unza.zm (و. موتامبو)